Volume 69, Issue 4, 2025

Journal of Scientific Research

of

The Banaras Hindu University

Properties of Tropical Mesoscale Convective Systems with respect to Prevailing Atmospheric Conditions over Southern Peninsular India

Anal Chandra Sarma*[1], Atri Deshamukhya[2], and Sanjay Sharma[3]

[1] Dept. of Physics, Patkai Christian College (Autonomous), Chumoukedima, Nagaland, Email: acspatkai@gmail.com
[2] Dept. of Physics, Assam University, Silchar, Assam, Email ID: atri.deshamukhya@gmail.com
[3] Principal, Dimapur Govt. College, Dimapur, Nagaland, Email ID: sanjay_sharma11@hotmail.com

Abstract: **The occurrence and intensity of convective cloud systems are greatly influenced by atmospheric conditions. A study has been carried to investigate the association between properties of Mesoscale Convective Systems and prevailing atmospheric conditions over southern peninsular India, a tropical area. Distinct seasonal and diurnal variations of the properties of MCSs, atmospheric convective parameters and their association have been observed. Monthly average occurrence of Mesoscale Convective Systems is found to be higher during south-west monsoon and is associated with higher precipitable water content. The deepest and strongest Mesoscale Convective Systems are found to occur during the pre-monsoon season during which locally developed instability and the local atmospheric conditions predominantly control the intensity of observed Mesoscale Convective Systems. During the south-west and the north-east monsoon, the intensity of Mesoscale Convective Systems over the region is predominantly controlled by the large scale atmospheric conditions. Over southern peninsular India though the Mesoscale Convective Systems are deeper during the north-east monsoon but they are relatively stronger in the south-west monsoon.**

Index Terms: **Mesoscale Convective Systems, monsoon, convective available potential energy, surface temperature, rainfall.**

I. Introduction

Mesoscale Convective Systems (MCSs) are mostly cumulonimbus cloud systems of different sizes and includes weather systems such as tropical cyclones, squall lines among others. MCSs occur with an ensemble of thunderstorms producing a contiguous precipitation area, with at least ~100 km or more in horizontal scale in one direction and have significant contribution to rainfall (Houze, 1993). They mainly emerge over the tropical area and represent 10% to 20% of total cloud population but associated with 70% to 80% of total observed rainfall over tropic (Mohr *et al.*, 1999; Nesbitt *et al.*, 2006; Roca *et al.,* 2014; Zhao, 2022). MCSs over tropical land are much more intense and show strong variability in comparison with tropical ocean (Nesbitt *et al.*, 2000, Peterson and Rutledge, 2001, Sharma *et. al.*, 2009). High intensity MCSs cause extreme weather events and frequency of such weather extremes has increased in last few decades and is projected to increase with climate change (Feng *et al.*, 2016; Taylor *et al.*, 2017; Schumacher & Rasmussen, 2020). Occurrence of MCSs over continental regions are influenced by orography of the region and are more frequent near mountain ranges (Morel and Senesi, 2002). In addition to an efficient triggering source such as a mountain ridge, strong diurnal heating and sufficient humidity at low level play important role in developing MCSs (Augustine *et al.*, 1989). In addition to strong thermodynamic environment such as high Convective Available Potential Energy (CAPE) and Surface Temperature (ST), factors like less Convective Inhibition (CIN) and strong wind circulation play important role in occurrence of MCSs (Bhowmik *et al.*, 2008).

The occurrence and intensity of convective cloud systems are greatly influenced by synoptic conditions such as daytime heating, moisture, pressure etc. Studies of favourable atmospheric conditions for MCSs are often region specific and 100 years of research on MCSs in different climate regimes of the world has highlighted how prevailing atmospheric conditions can impact initiation, development, and intensity of MCSs (Houze, 2018). In addition to an efficient triggering mechanism and favourable atmospheric conditions, formation of MCSs requires sufficient atmospheric instability (Doswell *et al.*, 1996; Schumacher & Johnson, 2005). Atmospheric instability can be studied in terms of atmospheric parameters like Convective

* Corresponding Author: Anal Chandra Sarma, Dept. of Physics
Patkai Christian College(Autonomous), Chumoukedima, Nagaland,
Email: acspatkai@gmail.com

Available Potential Energy (CAPE), Convective Inhibition (CIN), precipitable water etc. CAPE, CIN, moisture, temperature, low-level jet (LLJ), warm air advection etc. are important features for development of MCSs (Augustine and Caracena, 1994; Raymond *et al*., 2003). The presence of warm air advection at low-level (700 mb) prior to MCS initiation provides upward vertical motion in the atmosphere necessary for development of MCSs. Horizontal air flow at 850 mb which is a proxy for the LLJ, advects warm and moist air to help sustain the system. Occurrence of MCSs as well as rainfall from MCSs show positive correlation with CAPE (Adam and Souza, 2009; Sharma and Dutta, 2012). Region of atmospheric convection is characterized locally by substantial CAPE and low CIN above the boundary layer (Colby, 1984). The most Intense MCSs are often result of a interactions across synoptic as well as large scale atmospheric disturbances generating favourable environmental conditions for long lasting atmospheric convection (Schumacher & Johnson, 2005; Taylor *et al*., 2017; Latos *et al*., 2021; Vizy & Cook, 2022). Enhanced lower-level moisture, a warmer mid-troposphere, vertical wind shear etc. are associated with higher MCS precipitation (LeMone *et al*. 1998; Chen *et al*. 2023). An increase in sea surface temperatures (SST) leads to an increase in MCS occurrence over ocean but reduces it over land, while an elevated CO_2 level leads to an overall increase in MCS occurrence over ocean and land (Dong *et al*., 2025).

Several other studies have been carried out over the globe to study the association of atmospheric parameters with the strength of the convective systems (e.g. Doswell, 1987; Raymond *et al*. 2003; Houze, 2004; Geerts and Dejene 2005; Nicholls and Mohr 2010; Sohn *et al*., 2013; Ahmed & Schumacher, 2015; Chen *et al*. 2017; Klein *et al*., 2020; Baidu *et al*. 2022; Djakouré *et al*., 2024, Muetzelfeldt *et al*., 2025). Meteorological proxies like hail, lightning, rain intensity etc. are utilized to express the strength of the convective systems. Many works have been carried out to investigate the relation between the rain intensity and the atmospheric parameters (Fu *et al*., 1999; Eshel and Farrell, 2001; Agudelo et al, 2006; Myong and Gammon, 2010; Sohn *et al*., 2013, Jeong *et al*., 2016). In addition to meteorological proxies, radar and microwave imager derived proxies also can be utilized to study the intensity of the convective systems (Zipser *et al*., 2006; Liu & Liu, 2016; Zhang et al., 2025). In the present study attempt has been made to study the association of intensity of MCSs in terms of radar and microwave imager derived proxies with atmospheric parameters over southern peninsular India (8^0 – 16^0N and 73^0 – 80^0E). The study area receives rainfall during south-west monsoon as well as north-east monsoon. There are limited studies to investigate the association of radar and microwave imager derived proxies of convective intensity with the atmospheric parameters, over the globe in general and over the study region in particular.

II. DATA AND METHOD

In the present study, the number of occurrence and intensity of MCSs are obtained from data available from Tropical Rainfall Measuring Mission (TRMM) satellite. The sensors on board TRMM satellite are TRMM Microwave Imager (TMI), TRMM precipitation radar (TRMM-PR), Visible and Infrared Radiometer System (VIRS), Clouds and Earth's Radiant Energy System (CERES) and Lightning Imaging System (LIS). In the present study, TMI measured polarization corrected brightness temperature at 85 GHz (PCT_{85GHz}) is considered for the identification of MCSs while the vertical extent of the precipitation systems measured by TRMM-PR is considered as intensity of MCSs. Brightness temperature (T_b) is defined as the equivalent temperature of a black body that emits same intensity as measured for a target object (Ulaby *et al*., 1981). PCT_{85GHz} is an indicator of ice scattering within MCSs and lower value of this parameter indicates stronger convection. Precipitation systems are considered as MCSs, when they are characterized by an area of at least 2000 km^2 bounded by PCT_{85GHz} value of 250 ^{0}K, with a minimum value of PCT_{85GHz} in it $\leq$ 225 ^{0}K (Mohr and Zipser, 1996). TRMM-PR observations are mainly sensitive to liquid phase of hydrometeors and are attenuated by rain. The Echo Top Height of 20-dBZ TRMM-PR echo (ETH_{20dBZ}) is the maximum height of 20-dBZ radar reflectivity within the precipitation system. ETH_{20dBZ} indicates the vertical extent of precipitation-size ice particles i.e. how high the updraft can loft precipitation-size ice particles within the precipitation system (Xu and Zipser, 2012). On the other hand, the Echo Top Height of 40-dBZ TRMM-PR echo (ETH_{40dBZ}) is the maximum height of 40-dBZ radar reflectivity within the precipitation system. ETH_{40dBZ} indicates the vertical extent of the large precipitation-size particles such as graupel, hail etc. i.e. how high the updraft can loft these large precipitation-size particles within the precipitation system. ETH_{40dBZ} is a better indicator of convective intensity or updraft speed (Xu and Zipser, 2012). The observed MCSs are further categorized as deep convective systems (DCSs) with a criteria of $ETH_{20dBZ} \geq 14$ km (Liu and Zipser, 2005) and Intense Convective Systems (ICSs) with a criteria of $ETH_{40dBZ} \geq 10$ km (Houze *et al*., 2007).

The convective properties of the atmosphere have been studied in term of surface temperature, precipitable water content, Convective Available Potential Energy (CAPE), and Convective Inhibition Energy (CIN). Two parameters - surface temperature and precipitable water content are taken from NCEP and NCAR reanalyzed data product. These are "A" class data of NCEP and NCAR reanalyzed data product. Class A data is strongly influenced by the observed data and hence most reliable class. Two more atmospheric convective parameters - CAPE and CIN have been obtained from NOAA-CIRES 20th century reanalysed (version 2) data product. CAPE is the measure of potential instability in atmosphere while CIN is the measure thermodynamic stability. CIN can prevent convection even in presence of high CAPE.

MCSs and atmospheric convective parameters data during the years 1998-2013 are utilized for the present study. At first the climatology of the seasonal and diurnal variation of the properties of MCSs and associated atmospheric convective parameters has been studied. In order to find the association between the properties of MCSs and atmospheric convective parameters, near simultaneous and collocated values of the atmospheric convective parameters nearest to the centroid of the observed MCSs are considered. Further a correlation analysis is carried out between the MCSs parameters and the selected atmospheric convective parameters. The correlation coefficient (CC) between the MCSs and convective parameters are calculated by using the following formula

$$CC = \frac{\sum_{i=1}^{n}(M_i-\bar{M})(C_i-\bar{C})}{n\sqrt{\sum_{i=1}^{n}(M_i-\bar{M})^2\sum_{i=1}^{n}(C_i-\bar{C})^2}}$$

Here M_i is the MCS parameter, C_i is the convective parameter, $\bar{M}$ and $\bar{C}$ are their arithmetic mean and n is the number of data points.

III. Result and Discussion

Occurrence of MCSs shows distinct seasonal and diurnal variation over the study region. The monthly average percentage occurrence of MCSs is found to be highest (11.5%) during south-west monsoon months followed by north-east monsoon (9.67%) and pre-monsoon months (7.67%). However highest occurrence (16.5%) is seen in the month of October during north-east monsoon and minimum in the month of January as shown in Fig. 3.1(a). Increased atmospheric moisture and large scale atmospheric circulation play an important role in increasing the occurrence of MCSs during monsoon. Zheng *et al.*, (2008) reported occurrence of MCSs almost at any hour all the day during summer over China and its vicinity due to abundant moisture and favourable large-scale environment over Indian monsoon surge areas. Subrahmanyam *et al.*, 2019 reported that shallow, deep, and very deep convective clouds are abundant over Indian summer monsoon region. On diurnal scale maximum occurrence of MCSs is seen during the evening hours (16-20 hours), while the minimum occurrence of the same is seen during morning hours (8-10 hours) in all the three seasons. The maximum occurrence of MCSs during the evening hours may be attributed to the diurnal heating of low level of atmosphere (Chen & Houze, 1997; Morel & Sensei, 2002).

The frequency distributions of the intensity of MCSs in terms of maximum echo-top height with 20dBZ (ETH_{20dBZ}) and with 40dBZ (ETH_{40dBZ}) during the three seasons are shown in Fig. 3.1(b) and 3.1(c) respectively. In terms of ETH_{20dBZ}, the MCSs are found to be strongest during pre-monsoon (PM) followed by north-east monsoon (NEM) and south-west monsoon (SWM). The ETH_{20dBZ} is the vertical extent of the precipitation height and is an indicator of how high the updraft can lift precipitation-size ice particles (Xu and Zipser, 2012). In terms of ETH_{40dBZ}, the MCSs are found to be strongest during pre-monsoon followed by south-west monsoon and north-east monsoon. The ETH_{40dBZ} is the vertical extent of the large precipitation-size particles within the system, such as graupel, hail and is a better indicator of convective intensity or updraft speed of the convective cells (Xu and Zipser, 2012). The mean and standard

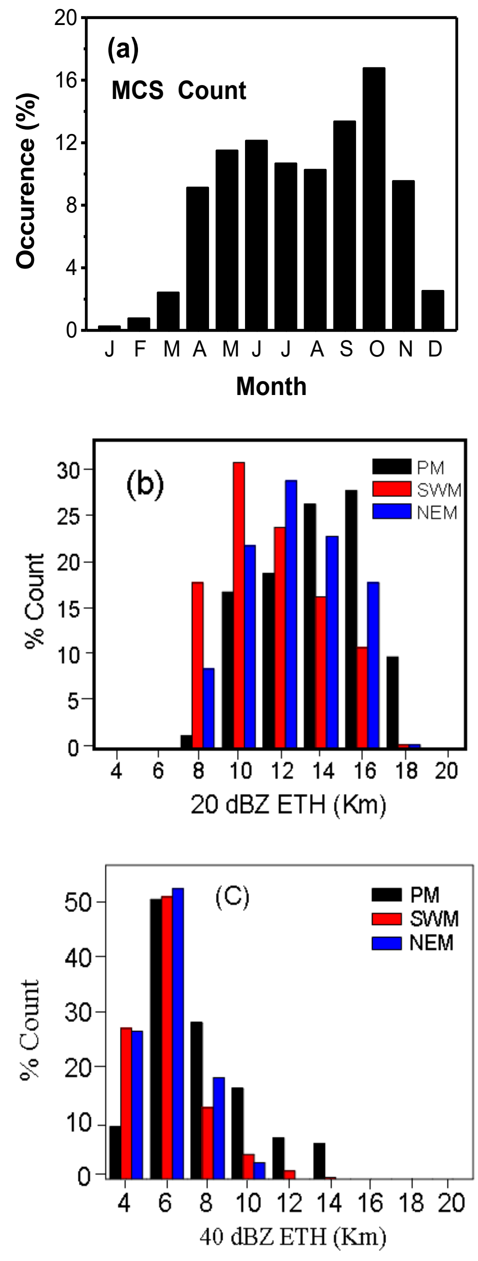

Fig. 3.1: Seasonal Variation of properties of MCSs (a) Occurrence (b) Maximum Echo Top Height at 20 dBZ (c) Maximum Echo Top Height at 40 dBZ

deviation (SD) of ETH_{20dBZ} and ETH_{40dBZ} are given in Table 3.1. Seasonally the deepest and strongest MCSs in terms of ETH_{20dBZ} and ETH_{40dBZ} respectively are observed in pre-monsoon month and can be attributed to highly unstable atmosphere due to surface warming and high temperature prevailing at lower levels in pre-monsoon season (Litta and Mohanty, 2008; Bhowmik *et al*., 2008). The mean values and frequency distributions of ETH_{20dBZ} and ETH_{40dBZ} during the three seasons suggest a paradox in the intensity of MCSs over southern peninsular India which shows that though the MCSs are deeper during the north-east monsoon by virtue of higher value of ETH_{20dBZ} but they relatively stronger in the south-west monsoon by virtue of higher value of ETH_{40dBZ}. The frequency distribution of ETH_{20dBZ} and ETH_{40dBZ} shows occurrence of deep convective systems (DCSs with a criteria of $ETH_{20dBZ} \geq 14$ km) during all the three seasons but occurrence of intense convective systems (ICSs with a criteria of $ETH_{40dBZ} \geq 10$ km) is found predominantly in pre-monsoon only. Maranan *et al*. (2018) also reported deepest, most organized MCSs in March–May (early first rainy season) and less organised MCSs with lower cloud tops in September–October period (second rainy season) over southern West Africa.

Table 3.1: Mean and SD of MCS parameters in pre-monsoon, SW monsoon and NE monsoon seasons

Parameter	Unit	Pre-monsoon		South-west monsoon		North-east monsoon	
		Mean (km)	SD (km)	Mean (km)	SD (km)	Mean (km)	SD (km)
ETH_{20}	km	13.98	2.45	11.53	2.45	12.69	2.34
ETH_{40}	km	08.04	2.80	06.00	1.70	05.93	1.31

Table 3.2: Mean and SD of MCS parameters during 00-06 hours, 06-12 hours, 12-18 hours and 18-24 hours

Season	**Parameter**		**00-06 hours**	**06-12 hours**	**12-18 hours**	**18-24 hours**
PM	ETH_{20dBZ}	Mean (km)	12.52	12.88	14.97	13.82
		SD (km)	2.59	2.48	2.15	2.36
	ETH_{40dBZ}	Mean(km)	6.23	6.13	8.80	8.21
		SD (km)	1.49	1.23	3.09	2.80
SWM	ETH_{20dBZ}	Mean(km)	10.77	10.84	12.10	2.80
		SD (km)	2.19	1.63	2.73	2.39
	ETH_{40dBZ}	Mean(km)	5.34	5.16	6.37	6.29
		SD (km)	1.31	1.10	1.96	1.64
NE M	ETH_{20dBZ}	Mean(km)	11.97	11.84	13.07	13.02
		SD (km)	2.27	2.32	2.09	2.50
	ETH_{40dBZ}	Mean(km)	5.43	5.05	6.10	6.35
		SD (km)	1.09	1.19	1.18	1.51

The mean and standard deviations of ETH_{20dBZ} and ETH_{40dBZ} during 00-06, 06-12, 12-18 and 18-24 hours in the pre-monsoon, south-west monsoon and north-east monsoon seasons are given Table 3.2. Distinct diurnal variations are seen in all the three seasons, the same being strongest in pre-monsoon. Diurnally MCSs are found to be stronger in the afternoon and evening hours in terms of both ETH_{20dBZ} and ETH_{40dBZ} during all the three seasons. The occurrence of the DCSs ($ETH_{20dBZ} \geq 14$ km), is also predominantly seen during the afternoon and evening hours, most significantly in the pre-monsoon season. In pre-monsoon season, CAPE and surface temperature are higher where as CIN is lower compared to other two seasons as given in Table 3.3. Because of surface warming and high temperature prevailing at lower levels, the atmosphere is highly unstable in pre-monsoon season (Litta and Mohanty, 2008; Bhowmik *et al*., 2008). The higher intensity of MCSs during the evening hours may be attributed to the diurnal heating of low level of atmosphere (Chen & Houze, 1997; Morel & Sensei, 2002).

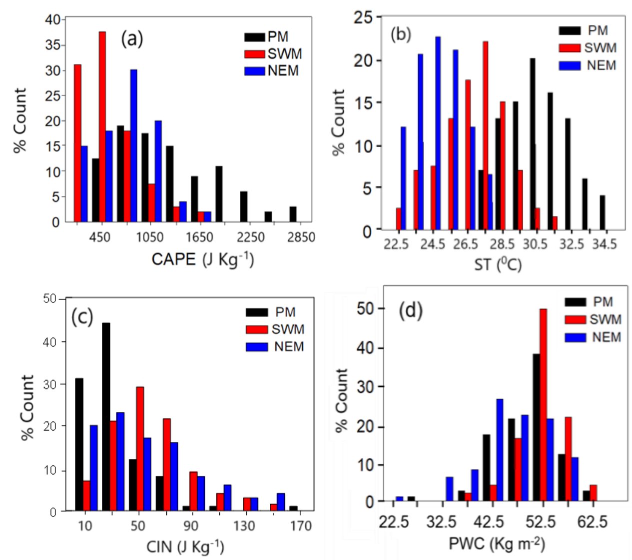

Fig. 3.2: Seasonal Variation of Atmospheric parameters (a) CAPE (b) Surface Temperature (c) CIN and (d) Precipitable water content

Using the TRMM observations, majority of the works over the South East Asia has been carried out to study the regional variability of the properties of the convective systems during the pre-monsoon and monsoon seasons only (Hirose and Nakamura, 2005; Houze *et al.*, 2007; Medina *et al.*, 2010; Romatschke *et al.,* 2010; Romatschke and Houze, 2011a; Romatschke and Houze, 2011b; Qie *et al.* 2014; Bhat and Kumar, 2015; Takahashi, 2016; Roy *et al*., 2017). The present study investigates the seasonal and diurnal variability of the properties of MCSs over the region during the pre-monsoon, south-east monsoon and north-east monsoon. The seasonal and diurnal variations MCS properties during the pre-monsoon and south-west monsoon are in agreement with the previous works carried out over the region according to which the MCSs during the pre-monsoon season are deeper and stronger compared to the south-west monsoon season (Romatschke *et al.,* 2010; Romatschke and Houze, 2011a; Romatschke and Houze, 2011b; Saikranthi *et al.,* 2014; Roy *et al*., 2017). The present study provides a new insight in the seasonal variability of MCS properties. It shows that, though the MCSs are deepest and strongest in the pre-monsoon season, but there is a paradox according to which though the MCSs are deeper by virtue of higher value of ETH_{20dBZ} during the north-east monsoon but they are stronger in the south-west monsoon by virtue of higher value of ETH_{40dBZ}.

The seasonal variations of atmospheric parameters nearest to the centroid of the observed MCSs at near simultaneous time scale are shown in Fig. 3.2 with the help of frequency distributions in terms of % count. The mean and SD of selected atmospheric convective parameters are given Table 3.3. Higher values of Convective Available Potential Energy (CAPE) and Surface Temperature (ST) are predominantly found during pre-monsoon. Mean values of these two parameters are highest in pre-monsoon followed by north-east monsoon and south-west monsoon. Convective Inhibition (CIN) is highest in south-west monsoon and lowest in pre-monsoon with a moderate value in north-east monsoon. Precipitable water content (PWC) is found to be higher in south-west monsoon with moderate values in north-east monsoon and pre-monsoon. Thus overall the three seasons are characteristically different in terms of atmospheric convective parameters. This result is in broad agreement with the result of Myoung and Gammon (2010), according to which the most significant atmospheric convective parameter with respect to precipitation varies by region and season, particularly over the continental region.

Table 3.3: Mean and SD of atmospheric convective parameters over southern peninsular India

Parameter	Unit	Pre-monsoon		SW monsoon		NE monsoon	
		Mean	SD	Mean	SD	Mean	SD
CAPE	J Kg^{-1}	1189	497	537	320	666	365
ST	^0C	29	4	25	2	26	2
CIN	J Kg^{-1}	35	22	64	38	56	37
PWC	Kg m^{-2}	49	6	53	5	46	7

ST: Surface temperature, PWC: Precipitable water content

Diurnal variations of atmospheric convective parameters are shown in Table 3.4 in terms of their mean and standard deviation during 00-06 hours, 06-12 hours, 12-18 hours and 18-24 hours. It shows higher value of CAPE in the evening hours (18-24 hours) in all the three seasons. Overall the pre-monsoon is found to be associated with higher values of CAPE and ST but lower value of CIN in comparison with other two seasons. No significant diurnal variation of PWC is found during the three seasons. Higher values of CAPE and ST result convectively unstable atmosphere suitable for MCS occurrence in pre-monsoon and in the evening hours in all the three seasons (Bhowmik *et al*., 2008). Atmospheric CAPE is expected to increase almost everywhere where as CIN is expected to increase over land due to global warming (Chen *et al*. 2020; Dong *et al*., 2024). This predicted increase in CAPE may result more frequent intense MCSs in future (Dong *et al*., 2024).

Table 3.4: Mean and SD of the atmospheric convective parameters during 00-06 hours, 06-12 hours, 12-18 hours and 18-24 hours

Season	Parameter		00-06 hours	06-12 hours	12-18 hours	18-24 hours
Pre-Monsoon	CAPE (J kg^{-1})	Mean	1018	1123	1237	1376
		SD	484	527	484	489
	ST (^oC)	Mean	27	28	30	29
		SD	3	3	4	4
	CIN (J kg^{-1})	Mean	47	27	35	28
		SD	24	20	19	22
	PWC (kg m^{-2})	Mean	51	50	49	47
		SD	7	8	7	4
SW Monsoon	CAPE (J kg^{-1})	Mean	457	325	531	623
		SD	537	277	292	385
	ST (^oC)	Mean	25	24	27	25
		SD	2	2	3	2
	CIN (J kg^{-1})	Mean	68	76	60	51
		SD	51	32	32	32
	PWC (kg m^{-2})	Mean	53	52	53	52
		SD	5	4	5	5
NE Monsoon	CAPE (J kg^{-1})	Mean	586	606	750	724
		SD	311	428	374	347
	ST (^oC)	Mean	24	25	26	25
		SD	2	2	2	2
	CIN (J kg^{-1})	Mean	58	71	44	51
		SD	37	46	32	34
	PWC (kg m^{-2})	Mean	45	49	46	47
		SD	8	8	6	6

Convectively unstable troposphere is a necessary but not sufficient condition for the development of convective systems. In an event of instability in a moist convection, lifting of an air parcel is a crucial factor for the development of the convective system (Doswell, 1987). Seasonally, the deepest and strongest MCSs in the pre-monsoon are associated with the higher values of CAPE, higher values of ST and smaller value of CIN. On the other hand, during south-west monsoon, MCSs are associated with lower values of CAPE, lower values of ST and higher values of CIN. Properties of MCSs during the north-east monsoon are associated with the moderate values of the selected atmospheric convective parameters. Highest monthly average occurrence of MCSs is found to be associated with comparatively higher value of PWC. In absence of thermal instability in atmosphere during monsoon as indicated by lower values of CAPE and ST but higher value of CIN, the occurrence of MCSs is influenced by PWC as a result of abundant moisture over the study area due to monsoon. This finding aligns with the study by Zheng *et al*., 2008 which reported frequent occurrence of MCSs due to abundant moisture and favourable large-scale environment prevailing over Indian monsoon surge areas. Klein *et al*., (2020) also reported less unstable, moist regime from June onward with increased MCS frequency over southern West Africa. They attributed this increased MCS frequency to total column water vapour. Diurnally, the deepest and most intense MCSs are found in the evening hours during the pre-monsoon and are associated with the maximum mean value of the CAPE, smaller value of CIN and higher mean surface temperature.

The quantitative association between the properties of MCSs and atmospheric convective parameters has been expressed in terms of correlation coefficient (CC). Overall the bulk parameter MCS count has highest correlation (CC = 0.76) with PWC while the intensity parameters are found to have better correlation with CAPE and surface temperature. Manzanilla and Miranda (2012) reported good correlations between MCS direction of motion and precipitable water content indicating significant influence of atmospheric moisture in occurrence of MCSs. Muetzelfeldt *et al*., (2025) reported that the total column water vapour among other environmental variables is a useful predictor of MCS occurrence. During the pre-monsoon season, the two selected intensity parameters ETH_{20dBZ} and ETH_{40dBZ} are found to have maximum correlation of 0.50 and 0.72 respectively with surface temperature. The significant correlation of MCSs parameters with surface temperature during the pre-monsoon suggests that the development of MCSs is initiated by locally developed instability and the local atmospheric conditions predominantly control the intensity of observed MCSs. During the south-west monsoon, ETH_{20dBZ} and ETH_{40dBZ} are found have maximum correlation of 0.51 and 0.40 respectively with CAPE. The correlations between the MCSs and atmospheric convective parameters during the north-east monsoon are found to be insignificant. During south-west and north-east monsoon, the occurrence of MCSs is found to be more in absence of local developed thermal instability indicated by lower CAPE and higher CIN. This is in contrast with the finding of Dong *et al*., (2024) according to which higher CIN contributes significantly to a decrease in MCS occurrence in presence of lower CAPE. The higher occurrence of MCS during monsoon in absence of local developed thermal instability and the relatively weak correlation of MCSs parameter with surface temperature during the south-west monsoon and insignificant correlation of MCSs parameter with surface temperature during the north-east monsoon suggests that the intensity of MCSs over the regions are predominantly controlled by the large scale atmospheric conditions during these two seasons, where the local atmospheric conditions contribute relatively less. While smaller scale processes like MCSs are difficult to predict in current global and climate models, larger scale process like Convectively Coupled Equatorial Waves(CCEWs) can be predicted with higher accuracy (Ying and Zhang, 2017; Dias *et al*., 2018; Judt, 2020). An observational understanding of how characteristics of MCSs are related to the large scale atmospheric conditions can be helpful for improve prediction of smaller scale processes like MCSs. Overall the seasonal variation in the correlation coefficient also suggests that the different mechanism play important role for the development of the MCSs in each season. The results of the present study are broadly in agreement with Myoung and Gammon (2010), Nicholls and Mohr (2010), Wang *et al*., (2014). Myoung and Gammon (2010) reported that the most significant atmospheric convective parameter with respect to precipitation varies by region and season, particularly over the continental region. Nicholls and Mohr (2010) reported that the value of the CAPE and some other atmospheric parameters were greater for the intense convective systems compared to the non intense convective systems. Wang *et al*., 2014 reported that compared with non-MCSs, environments of MCSs are often associated with large-scale atmospheric conditions.

Table 3.5: Seasonal variation of Association of MCS parameters with CAPE and surface temperature in terms of correlation coefficient (CC)

Season	Parameter	CC with	
		CAPE	ST
Pre-Monsoon	$ETH_{20\ dBZ}$	0.30	0.50
	$ETH_{40\ dBZ}$	0.37	0.72
SW Monsoon	$ETH_{20\ dBZ}$	0.51	0.28
	$ETH_{40\ dBZ}$	0.40	0.39
NE Monsoon	$ETH_{20\ dBZ}$	0.17	0.16
	$ETH_{40\ dBZ}$	0.13	0.12

CONCLUSION

The present study provides a comprehensive view of the seasonal and diurnal variation of the properties of MCSs and their association with atmospheric convective parameters over the southern peninsular India. A distinct seasonal and diurnal variation of the properties of MCS, atmospheric convective parameters and their association has been observed. Monthly average occurrence of MCSs is found to be higher during south-west monsoon and is associated with higher precipitable water content. The deepest and strongest MCSs are found to occur during the pre-monsoon season, the most convective season associated with the maximum mean surface temperature, moderate precipitable water content, maximum CAPE and minimum CIN. During the south-west monsoon, properties of MCSs are associated with lower values of CAPE, lower values of ST and higher values of CIN while during the north-east monsoon they are associated with the moderate values of the selected atmospheric convective parameters. This study shows a paradox in the properties of MCSs which suggests that though the MCSs are deeper during the north-east monsoon but they are stronger in the south-west monsoon. The occurrence of the deeper MCSs including the DCSs and stronger MCSs including the ICSs are found to be more during the evening hours in all the three seasons. The deepest and most intense MCSs are found to occur in the evening hours during the pre-monsoon season and are associated with the maximum mean value of the CAPE, smaller value of CIN and higher mean surface temperature.

Overall the bulk parameter MCS count has highest correlation (CC = 0.76) with PWC while the intensity parameters are found to have better correlation with CAPE and surface temperature with comparatively higher correlation during the pre-monsoon season. During the pre-monsoon the development of MCSs is initiated by locally developed instability and the local atmospheric conditions predominantly control the intensity of observed MCSs. During the south-west monsoon and the north-east monsoon the intensity of MCSs over the study region are predominantly controlled by the large scale atmospheric conditions. The results of the present study are broadly in agreement with previous studies and is expected to be helpful to understand the climatology of MCSs over the study region.

References

Adams, D.K., & Souza, E.P. (2009). CAPE and Convective Events in the Southwest during the North American Monsoon. *Mon. Wea. Rev.*, *137*, 83-98.

Agudelo, P.A., Curry, J. A., Hoyos, C. D., & Webster, P. J. (2006). Transition between suppressed and active phase of intra-seasonal oscillation in the Indo-Pacific warm pool. *J. Climate*, *19*, 5519-5530.

Ahmed, F., and C. Schumacher (2015). Convective and stratiform components of the precipitation-moisture relationship. *Geo phys. Res. Lett*., *42*, 10453–10462, https://doi.org/10.1002/2015 GL066957.

Augustine, J.A., Tollerud, E.I., & Jamison, B.D. (1989). Distributions and other general characteristics of mesoscale convective systems during 1986 as determined from GOES infrared imagery. In preprint volume, *12th Conference on weather analysis and forecasting* (Pp. 437–442), 2–6 October, 1989, Monterey, CA, USA.

Augustine, J.A., & Caracena, F. (1994). Lower-tropospheric precursors to nocturnal MCS development over the central United States. *Wea. Forecasting*, *9*, 116-135.

Baidu M., Schwendike J., Marsham J.H., and Bain C., (2022). Effects of vertical wind shear on intensities of mesoscale convective systems over West and Central Africa. *Atmos Sci. Lett*. 2022; 23: e1094. https://doi.org/10.1002/asl.1094

Bhatt, B.C., & Nakamura, K. (2005). Characteristics of monsoon rainfall around the Himalayas revealed by TRMM precipitation radar. *Mon. Wea. Rev*., *133*, 149-165.

Bhat, G.S., & Kumar, S. (2015). Vertical structure of cumulonimbus towers and intense convective clouds over the South Asian region during the summer monsoon season. *J. Geophy. Res.: Atmos*., *120* (5), 1710-1722.

Bhowmik S.K.R., Roy S.S. and Kundu P.K. (2008), Analysis of large-scale conditions associated with convection over Indian monsoon region. *Int. J. Climatology*, *28*, 797 821.

Chen, S. S. & Houze R. A. Jr. (1997). Diurnal variation and life-cycle of deep convective systems over the tropical Pacific warm pool. *Q. J. R. Meteorol. Soc*., *123*, 357-388.

Chen, B., Liu C., and Mapes B.E. (2017). Relationships between large precipitating systems and atmospheric factors at a grid scale. *J. Atmos. Sci.*, *74*, 531–552, https://doi.org/10.1175/JAS D-16-0049.1.

Chen, J., Dai, A., Zhang, Y., & Rasmussen, K., (2020). Changes in Convective Available Potential Energy and Convective Inhibition under Global Warming. Journal of Climate, 33, 2025-2050. https://doi.org/10.1175/JCLI-D-19-0461.1

Chen, X., L. R. Leung, Z. Feng, and Q. Yang, 2023: Environmental controls on MCS lifetime rainfall over tropical oceans. *Geophys. Res. Lett*., *50*, e2023GL103267, https://doi.org/10.1029/2023GL103267.

Colby, F.P. Jr. (1984). Convective inhibition as a predictor of convection during Ave-SESAME II. *Mon. Wea. Rev.*, *112*, 2239-2252.

Djakouré, S., Amouin, J., Kouadio, K.Y., & Kacou, M. (2024). Mesoscale Convective Systems and Extreme Precipitation on the West African Coast Linked to Ocean–Atmosphere Conditions during the Monsoon Period in the Gulf of Guinea. *Atmosphere*, *15*, 194. https:// doi.org/10.3390/atmos15020194

Dong, W., Zhao, M., Harris, Cheng, K.-Y., Zhou, L. & Ramaswamy, V. (2024). Contrasting Response of Mesoscale Convective Systems Occurrence Over Tropical Land and Ocean to Increased Sea Surface Temperature. *Geophy. Res. Lett*., *51* (21), e2024GL109251 https://doi.org/10.1029/2024GL109251

Dong, W., Zhao, M., Harris, L., Cheng, K.-Y., Zhou, L., & Ramaswamy, V. (2025). Response of global mesoscale convective systems to increased CO_2 and uniform SST warming in a global storm-resolving model. *Earth's Future*, *13*, e2024EF005776, doi: 10.1029/ 2024EF005776

Doswell, C. A. III (1987). The distinction between large scale and mesoscale contribution to severe convection: A case study example. *Wea. Forecasting*, *2*, 3-16.

Doswell, C.A.; Brooks, H.E.; Maddox, R.A. (1996). Flash Flood Forecasting: An Ingredients-Based Methodology. *Weather Forecast. 11*, 560–581.

Eshel, G., & Farrell, B. F. (2001). Thermodynamics of eastern Mediterranean rainfall variability. *J. Atmos. Sci, 58*, 87-92.

Feng, Z., Leung, L.R., Hagos, S., Houze,R.A., Burleyson, C.D., & Balaguru, K. (2016). More frequent intense and long-lived storms dominate the spring time trend in central US rainfall. *Nature Communications*, *7*(1), 13429 doi: doi.org/10.1038/ncomms13429.

Fu, R., Zhu, B., & Dickinson, R. (1999). How do the atmosphere and land surface influence the seasonal changes of convection in tropical Amazon?. *J. Climate*, *12*, 1306-1321.

Geerts, B., & Dejene, T. (2005). Regional and diurnal variability of the vertical structure of precipitation systems in Africa based on space borne radar data. *J. Climate, 18*, 893-916.

Hirose, M., & Nakamura, K. (2005). Spatial and diurnal variation of precipitation systems over Asia observed by TRMM Precipitation Radar. *J. Geophys. Res*., *110*, D05106. doi: 10.1029/2004JD004815.

Houze, R.A.Jr. (1993). Cloud Dynamics. *International Geophysics Series,* Academic Press*, 53*, 334.

Houze, R.A.Jr. (2004). Mesoscale convective systems. *Rev. Geophys*, *42*, RG4003, doi:10.1029/2004RG000150.

Houze,R.A. (2018). 100 years of research on mesoscale convective systems. *Meteorological Monographs*, *59*, 17.1-17.54. doi: 10.1175/AMSMONOGRAPHS-D-18-0001.1

Houze, R.A. Jr., Wilton, D.C., & Smull, B.F. (2007). Monsoon convection in the Himalayan region as seen by the TRMM Precipitation Radar. *Q. J. R. Met. Soc.*, *133*, 1389–1411.

Janiga, M.A., Schreck, C.J., Ridout, J.A., Flatau, M., Barton, N.P., Metzger, E.J., & Reynolds, C.A. (2018). Subseasonal forecasts of convectively coupled equatorial waves and the MJO: Activity and predictive skill. Mon .Wea. Rev., *146*. doi: 10.1175/MWR-D-17-0261.1

Judt, F. (2020). Atmospheric predictability of the tropics, middle latitudes, and polar regions explored through global storm-resolving simulations. J. Atmos. Sci., *77*, 257-276. doi: 10.1175/JAS-D-19-0116.1

Klein, C., Nkrumah, F., Taylor, C.M. & Adefisan, E.A. (2020) Sea sonality and trends of drivers of mesoscale convective systems in southern West Africa. *Journal of Climate*, *34*, 71–87.

Latos, B., Lefort,T., Flatau, M.K., Flatau, P.J., Permana, D.S., Baranowski, D.B., ... Schmidt, J.M. (2021). Equatorial waves triggering extreme rainfall and floods in south west Sulawesi, Indonesia. *Monthly Weather Review*, *149*(5), 1381-562 1401. doi: 10.1175/MWR-D-20-0262.1

LeMone, M. A., E. J. Zipser, and S. B. Trier, 1998: The role of environmental shear and thermodynamic conditions in determining the structure and evolution of mesoscale convective systems during TOGA COARE. *J. Atmos. Sci.*, *55*, 3493–3518.

Litta A.J. and Mohanty U.C. (2008), Simulation of a severe thunderstorm event during the field experiment of STORM programme 2006, using WRF-NMM model, Current Science, 95(2), 204-215.

Liu, N., & Liu, C. (2016). Global distribution of deep convection reaching tropopause in 1 year GPM observations. *J. Geophys. Res. Atmos.*, *121*, 3824–3842, https://doi.org/10.1002/2015JD024430.

Liu, C., & Zipser, E. J. (2005). Global distribution of convection penetrating the tropical tropopause. J. Geophys. Res.;Atmos., 110, D23104. doi:10.1029/2005D006063.

Manzanilla A. V. & Miranda V. L. B. (2012). Mesoscale convective systems during NAME. *Atmósfera*, *25* (2), 2012, 155-170

Maranan, M., A. H. Fink, & P. Knippertz, 2018: Rainfall types over southern West Africa: Objective identification, climatology and synoptic environment. *Quart. J. Roy. Meteor. Soc.*, *144*, 1628–1648, https://doi.org/10.1002/QJ.3345.

Medina, S., Houze, R.A. Jr., Kumar, A., & Niyogi, D. (2010). Summer monsoon convection in the Himalayan region: Terrain and land cover effects. Quart. J. Roy. Meteor. Soc., 136, 593-616.

Mohr, K.I., & Zipser, E.J. (1996). Defining mesoscale convective systems by their 85 GHz ice scattering signature. *Bull. Amer. Meteorol. Soc.*, *77*, 1179-1189.

Mohr, K.I., Famiglietti, J.S., & Zipser, E.J. (1999). The Contribution to Tropical Rainfall with respect to Convective System Type, Size, and Intensity Estimated from the 85-GHz Ice-Scattering Signature. *J. Appl. Meteor., 38*, 596-606.

Morel, C., & Senesi, S. (2002). A climatology of mesoscale convective systems over Europe using satellite infrared imagery. II: Characteristics of European mesoscale convective systems. *Q. J. R. Meteorol. Soc.*, *128*, 1973-1995.

Muetzelfeldt M. R., Plant R. S., Christensen H. M., Zhang Z., Woollings T., Feng Z, and Li P. (2025). Environmental Conditions Affecting Global Mesoscale Convective System Occurrence. *J. Atmos. Sci.*, *82* (2), 391-407. https://doi.org/10.1175/JAS-D-24 0058.s1.

Myoung, B., & Nielsen-Gammon, J.W.N. (2010). Sensitivity of Monthly Convective Precipitation to Environmental Conditions. *J. Climate*, *23*, 166-188.

Nesbitt, S.W., Zipser, E.J., & Cecil, D.J. (2000). A census of precipitation features in the tropics using TRMM: radar, ice scattering and lightening observations. *J. Climate*, *13*, 4087-4106.

Nesbitt, S.W., Cifelli, R., & Rutledge, S.A. (2006). Storm Morphology and Rainfall Characteristics of TRMM Precipitation Features. *Mon. Wea. Rev., 134*, 2702-2721.

Nicholls, S.D., & Mohr, K.I. (2010). An Analysis of the Environments of Intense Convective Systems in West Africa in 2003. *Mon. Wea. Rev., 138*, 3721-3739.

Petersen, W.A., & Rutledge, S.A. (2001). Regional variability in tropical convection: Observations from TRMM. *J. Climate*, *14*, 3566–3586.

Qie, X., Wu, X., Yuan, T., Bian, J., & Lu, D. (2014). Comprehensive Pattern of Deep Convective Systems over the Tibetan Plateau-South Asian Monsoon Region Based on TRMM Data. *J. of Climate*, *27*, 6612-6626.

Roca, R., J. Aublanc, P. Chambon, T. Fiolleau, and N. Viltard, 2014: Robust observational quantification of the contribution of mesoscale convective systems to rainfall in the tropics. J. Climate, 27, 4952–4958, https://doi.org/10.1175/JCLI-D-13 00628.1.

Romatschke, U., Medina, S., & Houze, R.A. Jr. (2010). Regional, seasonal and diurnal variation of extreme convection in the south asian region. *J. Climate*, *23*, 419-439.

Romatschke, U., & Houze, R.A. Jr. (2011a). Characteristics of precipitating convective systems in the pre monsoon season of south Asia. *J. Hydrometerol*., *12*, 157-180.

Romatschke, U., & Houze, R.A. Jr. (2011b). Characteristics of Precipitating Convective Systems in the South Asian Monsoon. *J. Hydrometerol, 12*, 3-26.

Raymond, D.J., Raga, G.B., Bretherton, C.S., Molinari, J., Lopez-Carrillo, C., & Fuchs, Z. (2003). Convective forcing in the intertropical convergence zone of the eastern pacific. *J. Atmos. Sci.*, *60*, 2064-2082.

Roy, P., Biswasharma, R., Deshamukhya, A., Sharma, S., & Gairola, R.M. (2017). A study of the spatiotemporal variability of the properties of intense precipitation features over the south Asian region: an integrated multi sensor approach. *Int. J. Climatology*, *37*, 624-639.

Saikranti, K., Rao, T.N., Radhakrishnan, B., & Rao, S.V.R. (2014). Morphology of the vertical structure of the precipitation over India and adjoining ocean based on long term measurements of TRMM-PR. *J. Geophy Res:Atmos*., *19*, 8433-8449. https://doi:org/10.1002/2014JD021774

Schumacher, R.S., & Johnson, R.H. (2005). Organization and environmental properties of extreme-rain-producing mesoscale convective systems. *Monthly Weather Review*, *133*(4), 961–976. doi: 10.1175/MWR2899.1

Schumacher, R.S., & Rasmussen, K.L. (2020). Theformation, character and changing nature of mesoscale convective systems. *Nature Reviews Earth & Environment*, *1*(6), 300–314. doi: 10.1038/s43017-020-0057-7

Sharma, S., Konwar, M., Sarma, D.K., Reddy, K.M., & Jain, A.R. (2009), Characteristics of rain integral parameters during tropical convective, transition and stratiform rain at Gadanki and its application in rain retrieval, *J. Appl. Meteorol. Climatol.*, *48*, 1245–1266.

Sharma, S., & Dutta D. (2012). Study of hail storm features in mesoscale convective systems over south east Asia by TRMM-precipitation radar and TRMM-microwave imager. *7th European Conference on radar meteorology and hydrology*, 25th to 29th June 2012, Toulouse, France.

Sohn, B. J., Ryu, G.-H., Song, H.-J. & Ou, M.-L. (2013). Characteristic features of warm-type rain producing heavy rainfall over the Korean Peninsula inferred from TRMM measurements, *Mon. Weather Rev*., *141*, 3873–3888.

Subrahmanyam, K., Kumar, K. K. & Reddy, N. N. (2019). New Insights into the Convective System Characteristics Over the Indian Summer Monsoon Region Using Space-Based Passive and Active Remote Sensing Techniques. IETE Technical Review, 37(2), 1-9. DOI: 10.1080/02564602.2019.1593890

Takahashi, H.G. (2016). Seasonal and Diurnal Variations in Rainfall Characteristics over the Tropical Asian Monsoon Region Using TRMM-PR Data. *SOLA*, *12A*, 22-27. Doi.10.2151/sola.12A-005

Taylor, C. M., Belusic, D., Guichard, F., Parker, D. J., Vischel, T., Bock, O., ... Panthou, G. (2017). Frequency of extreme sahelian storms tripled since 1982 in satellite observations. *Nature*, *544*(7651), 475–478. doi: 10.1038/nature22069

Ulaby, F.T., Moore, R.K., & Fung, A.K. (1981). *Microwave remote sensing: active and passive, Vol. I.* Artech House, Boston, London.

Vizy, E. K., & Cook, K. H. (2022). Distribution of extreme rainfall events and their environmental controls in the West African Sahel and Soudan. *Climate Dynam ics*, *59*, 997–1026. doi: doi.org/10.1007/s00382-022-06171-x

Wang C-C, Chieh-Sheng Hsu J, Tai-Jen Chen G, Lee D-I. (2014). A study of two propagating heavy-rainfall episodes near Taiwan during SoWMEX/TiMREX IOP-8 in June 2008. Part I: Synoptic evolution, episode propagation, and model control simulation. *Mon. Weather Rev*., *142*: 2619–2643.

Xu, W., & Zipser, E.J. (2012). Properties of deep convection in tropical continental, monsoon, and oceanic rainfall regimes. *Geophy. Res. Lett*., *39*(7), L07802. https://doi.org/10.1029/2012GL051242

Ying, Y., & Zhang, F. (2017). Practical and intrinsic predictability of multiscale weather and convectively coupled equatorial waves during the active phase of an mjo. J. Atmos. Sci., 74, 3771–3785.

Zhang, X., Ni, X., Dou, X., Xiao, H., and Ao, Y. (2025). Retrieval of Radar-Based Convection Intensity Parameters from Passive Microwave Observations via Machine Learning. *J. Atmos. Ocean. Tech*., *42*(7), 761-776. https://doi.org/10.1175/JTECH-D-24-0123.1

Zhao, M. (2022). A study of AR-TS-and MCS-associated precipitation and extreme precipitation in present and warmer climates. Journal of Climate, 35(2), 479–497. https://doi.org/10.1175/jcli-d-21-0145.1

Zheng, Y.G., Chen, J., & Zhu, P.J. (2008). Climatological distribution and diurnal variation of mesoscale convective systems over China and its vicinity during summer. *Atmos. Sc.*, *53*, 1574-1586.

Zipser, E.J., Cecil, D.J., Liu, C., Nesbitt, S.W., & Yorty, D.P. (2006). Where the most intense thunderstorms on earth?. *Bull. Amer. Meteorol. Soc., 87*, 1057–1071.

* * *